Article

Synthesis and Process Optimization of Electrospun PEEK-Sulfonated Nanofibers by Response Surface Methodology

Carlo Boaretti, Martina Roso, Alessandra Lorenzetti and Michele Modesti *

Department of Industrial Engineering, University of Padova, via Marzolo 9, 35131 Padova, Italy;
E-Mails: carlo.boaretti@dii.unipd.it (C.B.); martina.roso@unipd.it (M.R.);
alessandra.lorenzetti@unipd.it (A.L.)

* Author to whom correspondence should be addressed; E-Mail: michele.modesti@unipd.it;
Tel.: +39-049-827-5541; Fax: +39-049-827-5555.

Abstract: In this study electrospun nanofibers of partially sulfonated polyether ether ketone have been produced as a preliminary step for a possible development of composite proton exchange membranes for fuel cells. Response surface methodology has been employed for the modelling and optimization of the electrospinning process, using a Box-Behnken design. The investigation, based on a second order polynomial model, has been focused on the analysis of the effect of both process (voltage, tip-to-collector distance, flow rate) and material (sulfonation degree) variables on the mean fiber diameter. The final model has been verified by a series of statistical tests on the residuals and validated by a comparison procedure of samples at different sulfonation degrees, realized according to optimized conditions, for the production of homogeneous thin nanofibers.

Keywords: electrospinning; response surface methodology; sulfonated polyether ether ketone

1. Introduction

Nanofibers are an interesting and versatile class of one-dimensional nanomaterials, with diameters ranging from tenths to hundreds of nanometers, which have been recognized as promising due to their outstanding properties in terms of high porosity, excellent pore interconnectivity, small diameters and high surface-to-volume ratio. Among the different nanofiber manufacturing technologies, electrostatic

spinning, or electrospinning, represents the easiest, most promising [1] and versatile method for the generation of aligned or randomly distributed nanofibers of a rich variety of different materials, such as synthetic and natural polymers [2], composites [3], ceramics [4] and metals [5].

Electrospinning allows the production of nanofibers by applying a high electric field capable to overcome the surface tension of a polymeric solution. When the voltage reaches a threshold value the solution is deformed and produces an electrically charged jet that travels towards a grounded collector. During this phase the jet undergoes a whipping process in which it is stretched and, thanks to the evaporation of the solvent, produces a solid fiber. The morphology and diameter of the nanofibers obtained by this technique depend on a wide range of parameters whose effect can be dependent on the particular type of polymer/solvent system or can be influenced by the presence of interaction between two or more parameters. The intrinsicly-complex nature of the process does not always lead to satisfactory results from the applications of theoretical models, which can have limited descriptive capability, and prevent a full understanding of the results from a one factor analysis.

Response surface methodology (RSM) is a collection of statistical and mathematical techniques capable to allow the construction of an approximating model for the description of the relationship between a response and a set of predictor variables, on the basis of empirical data obtained by an appropriate experimental design. With RSM it is possible to carry out a simultaneous investigation of the effect of the single variables and their mutual interaction, with the possibility to define quantitatively optimized conditions to apply to a given process. In recent years, the application of this methodology for the optimization of the electrospinning process has encountered a growing interest [6–13], due to its easy implementation and the possibility to be adaptable to different polymer/solvent systems. Sulfonated polyether ether ketone (sPEEK) is a sulfonated derivate of the polyaryl ether ketone family, which has been recognized as a promising candidate for the replacement of Nafion for proton exchange membranes (PEMs) due to its good conductivity and thermal stability. In this context the employment of mechanically strong porous fiber matrix in composite PEMs represents one of the emerging and promising strategies to provide mechanical strength and promote dimensional stability [14]. A mat of homogeneous electrospun sPEEK nanofibers can provide a suitable reinforcing conductive matrix, whose properties can be tailored according to its sulfonation degree. Additionally, a very thin fibrous morphology is desirable because it can improve proton conductivity [15] or, in general, the electro-transport of ions through the alignment of the ionic groups along the fiber axis domain, probably due to the high shear forces responsible for the formation of thinner fibers. However, despite this potential interest towards the application of such fibers, up to date only few literature works have reported the electrospinning of sPEEK. Wang *et al.* [16] synthesized a sulfonated polyether ether ketone to produce core-shell nanofibers for gas sensing. Stated the poor inherently electrospinnability of the polymer, they coupled it with polyacrylonitrile in a weight ratio equal to 1:10 to produce nanofibers. Lee *et al.* [17] electrospun a composite nanofiber mat of SiO_2/sPEEK for fuel cell applications, starting from a solution of sPEEK and SiO_2 gel. They used very low flowrate (0.08 mL/h) and low relative humidity (below 15%) in order to obtain nanofibers. Chakrabarty *et al.* [18] have fabricated electrospun sPEEK nanofibers for electro-dialytic separation of Na^+ from Mg^{2+} or Ca^{2+} for potable water production. Choi *et al.* [19] realized a highly performant composite PEM made of sPEEK and carbon nanotube webs with a layer-by-layer deposition of such webs on electrospun sPEEK nanofibers subsequently fused by

solvent exposure, while Li *et al*. [20] incorporated nanosilver particles in nanofibers and nanospheres of a synthesized sPEEK for potential catalytic applications.

Apart from these few references no published work has been realized in order to explore and identify the best conditions for the electrospinning of sPEEK. The purpose of the present study is to provide a deeper insight regarding the electrospinning of sPEEK with a screening activity oriented to define the range of parameters employable to obtain homogeneous thin nanofibers. The results obtained from this study could thus be helpful as a preliminary step for the design of composite membranes for fuel cell or electrodialysis applications.

2. Experimental Section

2.1. Materials

Polyether ether ketone (PEEK) (M_w = 20,800 g/mol, density = 1.32 g/cm^3), sulfuric acid (95–97 wt % conc.), N,N-dimethylformamide (DMF), N,N-dimethylacetamide (DMAc), dimethylsulfoxide (DMSO) and 1-Methyl-2-pyrrolidinone (NMP) were purchased from Sigma-Aldrich (St. Louis, MO, USA).

2.2. Preparation of Sulfonated PEEK

PEEK beads were pulverized with an analytical mill and dried at 100 °C overnight to remove possible residual moisture. The sulfonation of PEEK (Figure 1) has been conducted according to the procedure developed by Huang *et al*. [21].
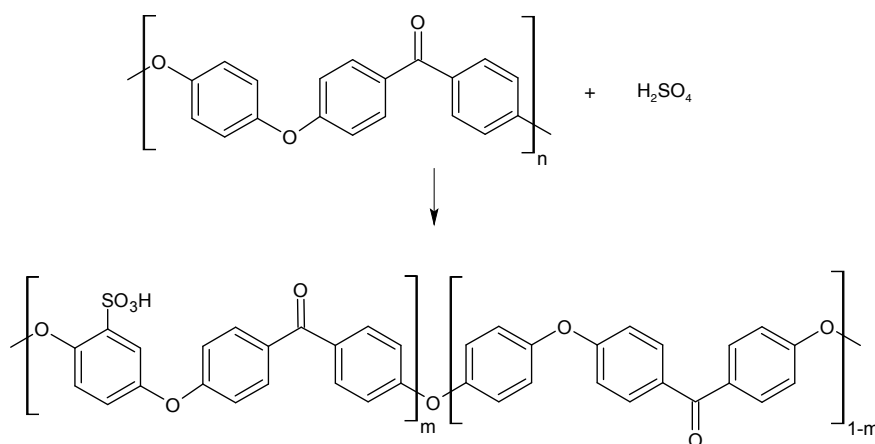

Figure 1. Sulfonation of PEEK.

Tests were carried at three different temperatures (45 °C, 55 °C and 65 °C), taking a sample from the reaction mixture every hour, up to a total of 5 h for each test. For every sample the polymer was recovered by precipitating the solutions in a five-fold volume of ice-cold deionized water. The suspensions were left in this state overnight and subsequently washed and filtered several times with deionized water until the pH of the rinsed water was as close as possible to neutral. After the removal of the acid residues the samples were dried in vacuum oven at 80 °C overnight and subsequently stored in a desiccator. The evaluation of the sulfonation degree (DS) of the samples was carried by titration. About 0.2 g of the samples were soaked in 100 mL of 0.1 M solution of NaCl, stirring the suspensions for 72 h to allow the

complete conversion of the material in its sodium salt form. Titration was carried out with a 0.01 N solution of NaOH, using phenolphthalein as an indicator. The uncertainty of the titration has been estimated at ±2% by the error propagation method. The evaluation of the ion exchange capacity (IEC) was carried according to the following equation:

$$IEC \left(\frac{meq}{g}\right) = \frac{V_{NaOH} \times C_{NaOH}}{W_{dry}} \tag{1}$$

where V_{NaOH} is the volume of NaOH solution consumed (mL), C_{NaOH} is the concentration of the NaOH solution (mol/L), and W_{sample} is the dry weight of the sample (g). The sulfonation degree, which quantifies the extent of the functionalization of the polymer, is defined as:

$$DS = \frac{moles_{sPEEK}}{moles_{sPEEK} + moles_{PEEK}} \tag{2}$$

while the moles of sPEEK and PEEK in 1 g of sulfonated polymer can be expressed as [22]:

$$moles_{sPEEK} = \frac{IEC}{1000} \tag{3}$$

$$moles_{PEEK} = \frac{1 - 0.001 \times IEC \times 369}{288} \tag{4}$$

where 369 and 288 are the molecular weights of the repetitive unit of sPEEK and PEEK in Daltons, respectively.

2.3. Solubility Evaluation

The evaluation of the sPEEK solubility was carried in different polar aprotic solvents commonly used for the dissolution of the polymer (DMF, DMAc, DMSO, NMP), according to the procedure of Gong *et al*. [23]. The judgment of the solubility was carried out by taking into consideration different sulfonation degrees and evaluating the results by a macroscopic inspection of the solutions.

2.4. Electrospinning Set-Up and Nanofibers Analysis

The electrospinning experiments have been carried out with a conventional apparatus, composed of a syringe pump, a variable DC power supply, and a metal rotating collector in order to obtain a uniform distribution of the fibers. A common 6 mL plastic syringe (Terumo) was mounted on the syringe pump (Harvard 11 Pico Plus Syringe Pumps) and fitted with a 27G (Terumo, 0.4128 mm o.d, 0.21 mm i.d.) stainless steel hypodermic needle. A variable DC power supply (Gamma High Voltage, Ormond Beach, FL, USA) was used to produce a potential difference in the range of 0–30 kV. The positive (anode) terminal was connected to the stainless steel needle using a steel spring-loaded clip with serrated jaws (alligator clip), while the ground (negative) terminal of the power supply (cathode) was attached to the rotating metal collector. The electrospinning apparatus was enclosed in a PMMA sealed chamber to electrically insulate the system, to avoid air currents and maintain a stable environment. All the tests have been conducted in a monitored environment, where both temperature and humidity were measured constantly. The polymeric solutions were prepared by dissolving the samples overnight at room

temperature in the selected solvents under intense stirring. The morphology of the electrospun samples was characterized by scanning electron microscopy (SEM) (JSM 6490, Jeol Ltd., Tokyo, Japan) micrographs of gold-sputtered samples deposited on aluminum foil. Fibers were measured by image analysis with ImageJ software (version 1.48), taking a total of 200 diameters for each sample from different photos.

2.5. Variables and Design Selection

The best conditions for the electrospinning of sPEEK were identified by conducting a preliminary screening activity with a one-factor-at-a-time approach, considering both solution and process variables. During this first phase, the aim was to identify a proper choice for the solvent and polymer concentration and define a suitable range for the other variables considered, in order to have a stable electrospinning process and a uniform fiber morphology. Once that those conditions were identified, the second part of the study has been characterized by an experimental campaign based on a Box-Behnken Design (BBD) [24,25]. In this case, to approximate the relationship between the response and the different variables selected, a second-order linear model has been built according to the following general equation [26]:

$$y = \beta_0 + \sum_{i=1}^{k} \beta_i x_i + \sum_{i=1}^{k} \beta_{ii} x_{ii}^2 + \sum \sum_{i<j}^{k} \beta_{ij} x_i x_j + \varepsilon_{ij} \tag{5}$$

where y is the response of the design, x_i and x_j are the components of the vectors corresponding to the different coded levels of the variables selected, k is the number of variables, β_i and β_{ii} are the coefficients associated to the linear and quadratic levels of the single variables while β_{ij} is the coefficient associated to the interaction between pairs of variables. The term ε_{ij} represents the statistical error associated to the model, assumed to be an independent and identically-distributed random variable. The previous expression makes use of coded levels of the variables which can be obtained by a simple transformation, using the minimum and maximum values of the natural variables (z_i) selected [27]:

$$x_i = \frac{z_i - (\max(z_i) + \min(z_i))/2}{(\max(z_i) - \min(z_i))/2} \tag{6}$$

This coding procedure is widely used for the fitting of linear regression models because all the variables become dimensionless and their values fall between −1 and +1, allowing a better comparison between the relevance of variables that, in their natural state, have different orders of magnitude and units of measure. The present study is based on 4-variables-3-level BBD for the evaluation of the effect of the following four variables: voltage, flow-rate, tip-to-collector distance, and sulfonation degree. The choice of these variables has been done in order to evaluate the effect of the process parameters, which could be specific for a given polymer/solvent system, and the effect of the sulfonation degree on the final morphology and dimension of the nanofibers. The influence of the solution concentration has not been screened in depth because it can be predominant over other factors and its effect on the final morphology of the fibers is generally accepted and widely reported in the scientific literature [28–30]. In this regard the choice has been to select a concentration value capable to produce good and uniform nanofibers and keep it constant at that specific value. For this number of factors and levels taken into

consideration the choice of a BBD is more convenient, since it possesses features very similar to a classic Central Composite Design but requires a lower number of runs, avoiding the employment of axial runs and with the possibility of using only three evenly-spaced levels of the variables. The statistical analysis of the experimental data has been conducted by employing Design Expert software (trial version 9.0.2, Stat-Ease), using the mean fiber diameter and their standard deviation as response variables. The statistical tests for the diagnostic of the developed model have been carried with *R* (The *R* Foundation for Statistical Computing, version 3.1.2).

3. Results and Discussion

3.1. PEEK Sulfonation

According to the scientific literature [31,32], the most commonly used equation to express the aromatic sulfonation rate in aqueous sulfuric acid is the following:

$$-\frac{\mathrm{d}[Ar]}{\mathrm{d}t} = k[Ar]\frac{A_{\mathrm{H_2SO_4}}^2}{A_{\mathrm{w}}} \tag{7}$$

where $[Ar]$ = concentration of the aromatic ring to be sulfonated, $[H_2SO_4]$ = concentration of sulfuric acid, A_{w} = activity of water (proportional to the concentration of water in the system), k = reaction rate constant and t = reaction time. Sulfonation gives a better yield at elevated temperatures, especially in the case of sulfonation to higher levels. In addition, the concentration of the sulfuric acid or oleum used as the sulfonating agent influences the course of the reaction. Sulfonation prefers high concentrations of sulfonating agents, while water, formed as a byproduct, reduces the rate of the reaction [21,33]. The sulfonation of PEEK is an electrophilic aromatic substitution reaction in which the sulfonic acid groups take place preferentially in one of the four position of the aromatic ring between the ether linkages of the polymer repetitive unit, while the other two aromatic rings have low electron density due to the electronic withdrawing effect of the adjacent carbonyl group [21]. The results of the experimental tests at different temperatures are reported in Figure 2. As expected the kinetics improves by increasing the temperature and generally shows a logarithmic relationship with time. The kinetics of the reaction has been described with the model proposed by Shibuya and Porter [34,35], assuming a negative effect of the sulfonated aromatic ring on the rate expression:

$$-\frac{\mathrm{d}c}{\mathrm{d}t} = \frac{k_1 c}{k_{\mathrm{d}}(c_0 - c)} \tag{8}$$

where c = concentration of the substrate (aromatic ring to be sulfonated) at time t, c_0 = initial substrate concentration, k_1 = rate constant of sulfonation, k_{d} = rate constant for the negative effect of the sulfonated ring. By integration the equation becomes linear over time:

$$c_0[-X - \ln(1 - X)] = Kt \tag{9}$$

where X represents the reaction conversion (or sulfonation degree) and K is the ratio between k_1 and k_d. By converting the experimental data according to this formula it was possible to observe that they fall along a line (Figure 3a), proving the coherence of the postulated model.
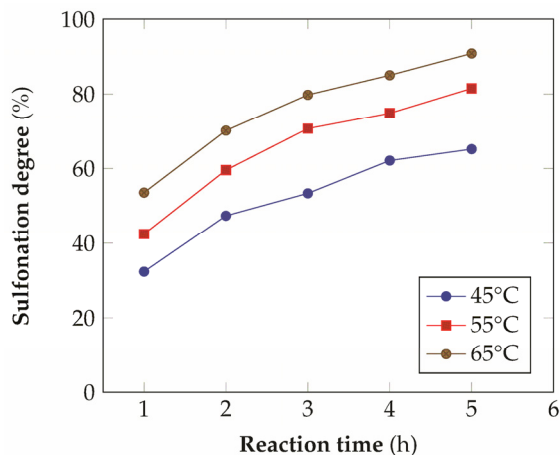
Figure 2. Degree of sulfonation of PEEK in concentrated H_2SO_4 as a function of time and temperature (onset of the time scale is from the complete dissolution of the polymer in acid).

In this manner, from the slopes of the linear approximation, it has been possible to obtain the ratio k_1/k_d (Table 1), which can be used to re-fit the experimental data. The final fitting (Figure 3b) seems quite satisfactory for the relatively low number of experimental points taken into consideration and it has been proved to be more reliable with respect to other kinetics expressions that don't account for the deflator effect [21].
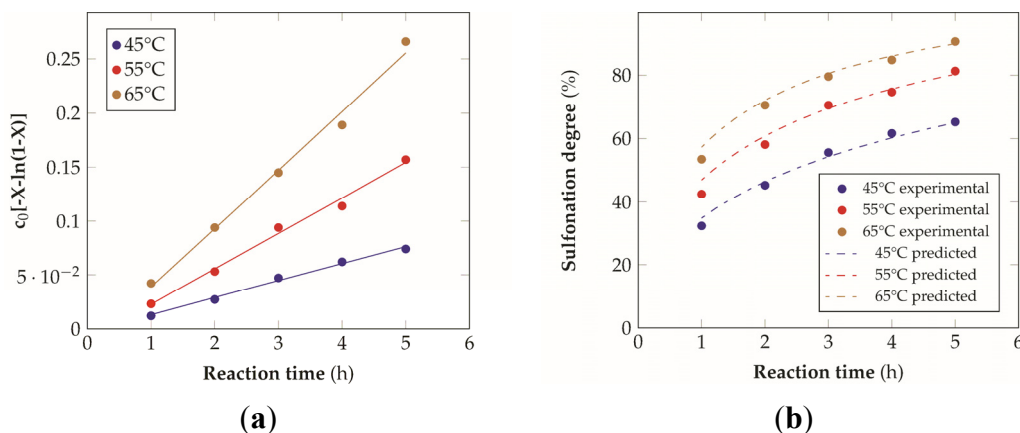

(a)

(b)

Figure 3. Kinetic modeling of the sulfonation reaction: (**a**) linearization of the kinetic expression as a function of time, (**b**) comparison between the experimental data and the model prediction ($R^2 = 0.98$ for the data at 45 °C, $R^2 = 0.97$ for the data at 55 °C, $R^2 = 0.99$ for the data at 65 °C).

Table 1. k_1/k_d ratio obtained at different temperatures.

Temperature (°C)	C_0 (mol/L)	k_1/k_d (mol/L·h)
45	0.183	0.0146
55	0.183	0.0308
65	0.183	0.0507

The values of the kinetic parameters obtained from this analysis are thus useful to predict the time required to attain a given sulfonation degree of the polymer, according to one of the selected temperatures.

3.2. sPEEK Solubility

PEEK is generally highly resistant to dissolution in most common solvents and for this reason its solubility is generally limited to harsh solvents, especially strong acids like H_2SO_4, CH_3SO_3H and HSO_3Cl, which also act as reagents for its sulfonation [26]. Upon sulfonation the polymer becomes progressively more polar with the increase of the sulfonation degree and can also be dissolved in polar aprotic solvent with high dielectric constants. The solubility is not only a function of the sulfonation degree but also of the concentration in the solution, which is mainly related to the molecular weight of the polymer. A good solubility is necessary for electrospinning in order to have a stable solution during the entire process for the production of the nanofibers. As can be seen from Table 2, to allow a complete solubility in the solvents employed, a sulfonation degree of at least 55% is necessary. However, different behaviors can be identified. For example DMSO and NMP seem to be able to interact more significantly with the polymer at low sulfonation degrees, probably due to their high polarity. On the basis of the data obtained from the reactions, three samples with a sulfonation degrees of about 60%, 70% and 80% were taken into consideration for the subsequent analysis. These sulfonation degrees correspond, respectively, to the samples sulfonated for two and three hours, at 55 °C, and for three hours, at 65 °C.

Table 2. Solubility of different sPEEK samples in different organic solvents (Sw. = swelling, + = partial solubility, ++ = complete solubility).

Sulfonation Degree	DMF	DMAc	DMSO	NMP
33%	Sw.	Sw.	Sw.	Sw.
45%	Sw.	Sw.	+	+
50%	+	+	+	++
≥ 55%	++	++	++	++

3.3. Electrospinning Screening

A first assessment to define the proper conditions for the electrospinning of the sulfonated polymer has been carried out in order to identify the best solution concentration/solvent coupling to produce homogeneous nanofibers. Due to the low molecular weight of the polymer high concentrations are required in order to have a sufficient viscosity to allow the stretching of the solution and the formation of a stable Taylor cone. For this reason the concentration range investigated was between 20 and 30 wt % and the results are shown in Table 3. As can be seen the morphologies of the samples are influenced by the solvent chosen for a given concentration of the polymer solution.

Generally speaking, a concentration of at least 25% by weight of polymer in the solution is required for the formation of fibers, with the only exception for the solutions with NMP, for which the minimum concentration is 27% by weight. Below these values the fibers are highly heterogeneous, with the presence of beads or a significant beads-on-fibers morphology. On the other hand even a concentration of about 30% by weight is not recommended since the morphology changes, leading to the formation of ribbons. This is true except for the case of NMP solutions, for which it appears clear that the concentration interval for stable nanofibers is slightly higher than for the solutions of the other solvents. A possible explanation for this is related to the properties of the solvent. NMP possesses a high surface tension coupled to a high boiling point, compared to the other solvents chosen. This probably leads to a

slower rate of solvent evaporation and the necessity to have a higher polymer concentration to increase the viscosity of the solution. Indeed at a concentration of 25 wt % the fibrous morphology is present but with a high concentration of defects. A comparison was also made by employing binary mixtures of the selected solvents in a 50:50 weight ratio. In this case a concentration of about 27 wt % was chosen, since it could be considered the value at which most of the solvents could produce a homogeneous fiber morphology.

Table 3. Morphology of the electrospun samples obtained during the screening phase (sulfonation degree ≈ 70%, electrospinning condition: voltage = 20 kV, distance: 14 cm, flow-rate: 0.125 mL/h).

Solution Concentration	Solvent			
	DMF	**DMAc**	**DMSO**	**NMP**
20 wt %				
25 wt %				
27 wt %				
30 wt %				

The results showed that the best morphology can be obtained by mixing DMF with DMAc (Figure 4a). Only in this case the properties of the solvents and the polymer concentration can lead to the formation of smooth and quite uniform fibers. The samples, electrospun with the DMF/NMP (Figure 4c) and DMAc/NMP (Figure 4f) mixtures, present a beads-on-fiber morphology that gives fibers high non-uniformity. Despite the fact that at a 27 wt % concentration the solution with only DMSO as solvent produced ribbons instead of fibers, some samples of the mixture with DMSO were realized. Mixing DMSO with DMAc (Figure 4d) at the given concentration, it is possible to produce fibers, even though they seem irregular with significant variation of the diameter along a single fiber. The DMSO/NMP (Figure 4e) samples presented the worst morphology due to the presence of both beads along fibers and branched jets, in which smaller jets were formed on the surface of primary jets.
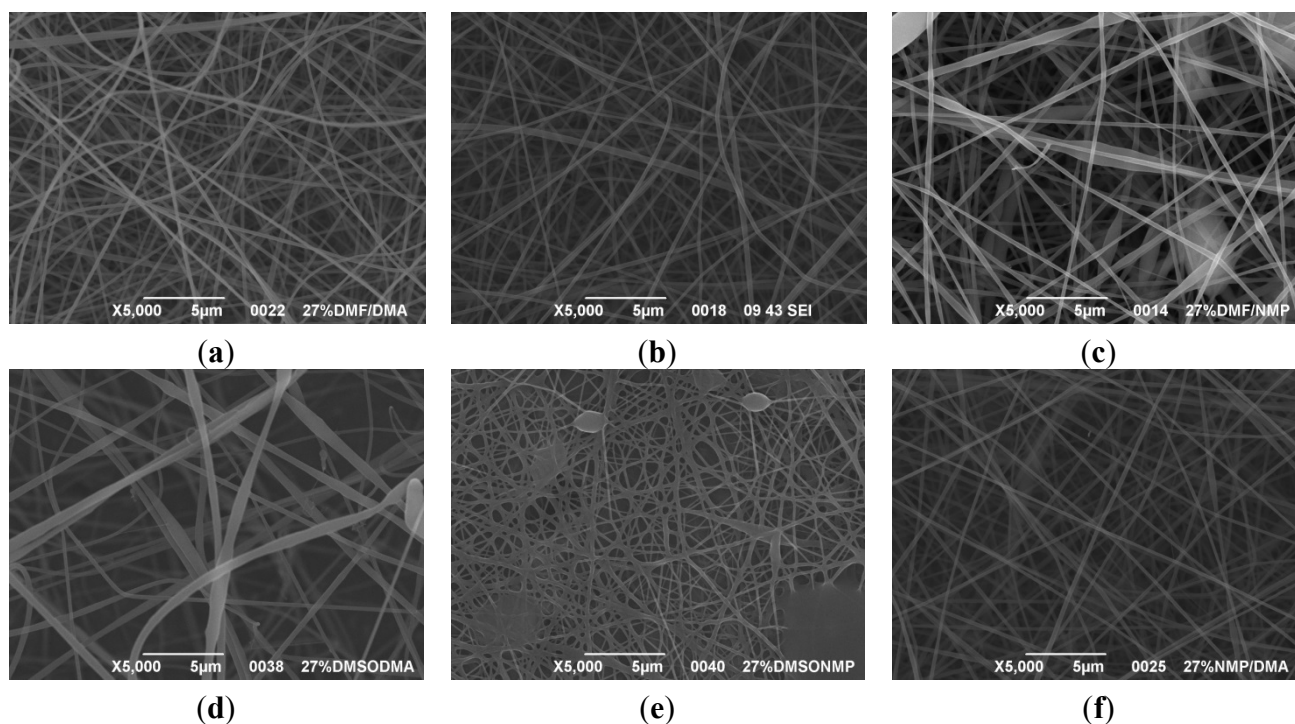
Figure 4. SEM micrographs of polymer solutions with binary mixture (50:50 w/w) of solvents (sulfonation degree DS ≈ 70%, electrospinning condition: voltage = 20 kV, distance: 14 cm, flow-rate: 0.125 mL/h): (**a**) DMF/DMAc; (**b**) DMF/DMSO; (**c**) DMF/NMP; (**d**) DMSO/DMAc; (**e**) DMSO/NMP; (**f**) NMP/DMAc.

From this first screening activity it has been possible to draw some preliminary conclusions regarding the operative conditions to employ in order to obtain a stable and uniform fiber morphology of the electrospun solutions. First, it is important to operate with low flow rates, usually with a maximum values of 0.2 mL/h. This is necessary in order to obtain the production of a uniform deposition of fibers since, with high flow rates, the process is not stable with a common range of voltages and it is likely to result in the spraying of solution droplets from the tip of the syringe. In some cases, depending on the type of solvent employed, even higher flow rates (0.4 mL/h) are employable, but this seems not to be a good choice since, even if at the beginning the process is stable, once that a given amount of fibers are produced and a small layer of mat is deposited, it probably acts as an insulating layer that decreases the potential difference between the two electrodes, with a final effect that is comparable to a decrease in the applied voltage. On the other hand it is also important to define a proper range of values for the voltage. A good choice is to use voltages that are not lower than 15 kV, unless to employ a very low tip-to-collector distance; otherwise, the spinning process is not stable over time. A maximum value of 30 kV has been chosen, which is usually the full-scale value for high-voltage supplies commonly employed for electrospinning, and for safety reasons. The distances from the tip to the collector were chosen by considering the necessity to provide a sufficient time of flight of the jet in order to stretch and evaporate the solvent, for the lower level, and to be capable both of reaching the collector and to be subjected to a sufficient electric strength in order not to generate drips, for the higher level. The conditions that satisfied these requisites were defined in terms of 10 cm for the lower value and 18 cm for the higher. Although not controlled to a specific level, it has been identified that relative humidity

plays an important role for the electrospinning of the polymer. Best conditions are achieved at low levels of humidity; otherwise, the deposition of the fibers is problematic and the nanofibers tend to form yarns (Figure 5a), which subsequently aggregate to form a bundle (Figure 5b) from the tip electrospinning of other sulfonated polymers [36] and ionomers [37,38]. The choice of the solvent to be employed is another important aspect to define. The experimental tests have shown that DMF and DMAc, or a combination of the two, could be good choices for the possibility of having a wider range of solution concentrations, lower surface tensions and boiling points.
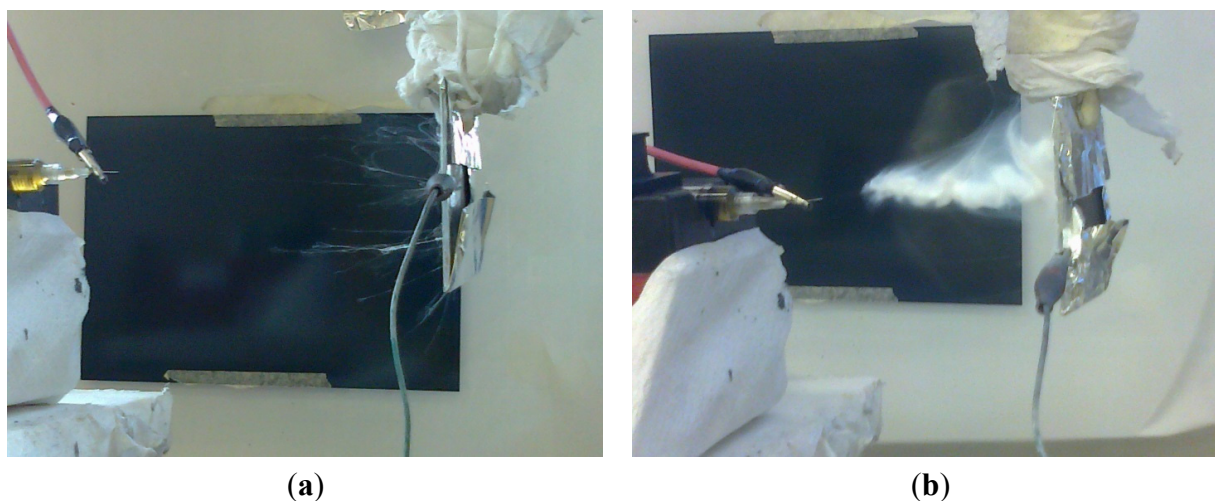

| (**a**) | (**b**) |

Figure 5. Progressive formation of nanofiber yarns in conditions of high relative humidity: (**a**) at the beginning and, (**b**) after several minutes of electrospinning.

The final conditions identified for a possible optimization of the sPEEK electrospinning have been subsequently evaluated in depth with a statistical analysis based on the design of experiments (DoE) approach in order to better identify which conditions can be employed to obtain high quality nanofibers.

3.4. The Box-Behnken Design

Once identified the conditions to allow a stable electrospinning process of the polymer, the following step has been the determination of the variables' influence on the fiber dimension by the employment of a 4-variables-3-levels BBD. The solvent selected was DMAc, while the solution concentration was fixed at the value of 26 wt %, since it has been identified as the lower value capable to produce fibers without defects. Each run has been carried under controlled environmental conditions, with a relative humidity below 30% and 21.3 ± 0.5 °C of temperature. The values of the other variables are reported in Table 4. The experimental design consisted in 29 runs with 5 repetitions in the center point (Table 5).

Table 4. Variables chosen for the designed experiment.

Variable	Symbol	Lower Value	Center Value	Upper Value
Sulfonation degree (%)	A	60	70	80
Voltage (kV)	B	20	25	30
Distance (cm)	C	10	14	18
Flow rate (mL/h)	D	0.050	0.125	0.200
Coded value	–	−1	0	+1

Table 5. Experimental matrix for the Box-Behnken design.

Run #	A (%)	B (kV)	C (cm)	D (mL/h)	Mean (nm)	Std. Dev. (nm)
1	60	20	14	0.125	181	32
2	80	25	10	0.125	166	35
3	70	25	14	0.125	164	29
4	70	20	14	0.200	167	35
5	80	25	14	0.200	205	50
6	80	25	14	0.050	192	32
7	60	25	10	0.125	218	50
8	70	30	14	0.050	182	36
9	70	25	14	0.125	167	25
10	70	25	14	0.125	171	28
11	70	20	18	0.125	179	38
12	70	20	14	0.050	189	34
13	60	25	14	0.200	193	27
14	70	30	18	0.125	190	45
15	70	25	14	0.125	167	25
16	70	25	10	0.200	184	40
17	60	25	18	0.125	199	33
18	60	60	14	0.125	187	32
19	70	25	18	0.050	225	40
20	70	25	14	0.050	201	55
21	80	25	18	0.125	222	54
22	70	25	18	0.200	216	60
23	70	30	10	0.125	172	38
24	70	25	14	0.125	170	29
25	70	30	14	0.200	182	35
26	80	20	14	0.125	170	33
27	80	30	14	0.125	171	31
28	70	30	10	0.125	173	37
29	60	25	14	0.050	233	46

The sequence of the runs were randomly defined by the software in order to highlight possible external influences not taken into consideration in the design. The results of the image analysis have shown that the variation of the variables selected produced mean fiber diameters ranging from about 165 to 235 nm and standard deviations ranging from 25 to 60 nm.

3.5. Analysis of the Mean Fiber Diameter

The first step in the evaluation of the response of the design has been carried by conducting an analysis of variance (ANOVA) (Table 6), as a preliminary phase in the construction of a second-order model to describe the response surface for the fitting of the experimental data. With this approach the statistical significance of each variable selected and the possible interactions between them were evaluated with a backward elimination method by retaining only those terms with a *p*-value $\leq$ 0.05 to reduce the complexity of the polynomial expression.

Table 6. ANOVA for response surface reduced quadratic model of the mean fibers diameter (SS = sum of squares, D_f = degrees of freedom, MS = Mean squares).

Source	SS	D_f	MS	*F*-Value	*p*-Value
Model	11782.88	11	1071.17	140.13	<0.0001
A-DS	720.75	1	720.75	94.29	<0.0001
B-Voltage	133.33	1	133.33	17.44	0.0006
C-Distance	1102.08	1	1102.08	144.17	<0.0001
D-Flow rate	481.33	1	481.33	62.97	<0.0001
AC	1369.00	1	1369.00	179.09	<0.0001
AD	784.00	1	784.00	102.56	<0.0001
BD	121.00	1	121.00	15.83	0.0001
A^2	1891.17	1	1891.17	247.40	<0.0001
B^2	502.31	1	502.31	65.71	<0.0001
C^2	2003.55	1	2003.55	262.10	<0.0001
D^2	3125.21	1	3125.21	408.84	<0.0001
Residual	129.95	17	7.64	–	–
Lack of fit	96.75	13	7.44	0.90	0.6090
Pure error	33.20	4	8.30	–	–

The estimation of the coefficients of the linear regression model was determined by a least square minimization. The final refined model excluded the presence of the interaction terms AB and BC, leading to the following final equation in terms of coded factors:

$$Md = 167.60 - 7.75 \times A + 3.33 \times B + 9.58 \times C$$

$$- 6.33 \times D + 18.50 \times AC + 14.00 \times AD$$

$$+ 5.50 \times BD + 17.07 \times A^2 - 8.80 \times B^2$$

$$+17.58 \times C^2 + 21.95 \times D^2$$

(10)

The adequacy of the regression model chosen for the description of the experimental results has been confirmed by the value of 0.98 for the determination coefficient (R^2) and the not significant lack of fit (*p*-value = 0.6), with respect to the pure error. The obtained ratio of 40.062 for the adequate precision, which measures the signal-to-noise ratio, is greater than 4 and indicates that the model can be used to navigate in the design space. All the factors selected for the design have proven to be important in the description of the variability in the data, although with different extents. Indeed, from the analysis of the relative importance of the different regressors on the determination coefficient (Figure 6), voltage has been identified as the factor that has less relevance with respect to the other terms of the model for both its first-order, interaction and quadratic terms.

A similar result has been previously noted for the electrospinning of *Bombyx mori* silk [6] and PAN [8] in relation to the employment of solutions with an high polymer concentration although the opposite result has been found for the electrospinning of Poly(D,L-lactide) [7], probably due to a low tip-to-collector distance [8]. Between the terms of different order the quadratic component is the most significant for the prediction of the data, with a total contribution of about 60%. This result indicates the presence of strong

curvature and optimal conditions probably not far from the center of the design space, in agreement with the assumptions on which the BBD is based.
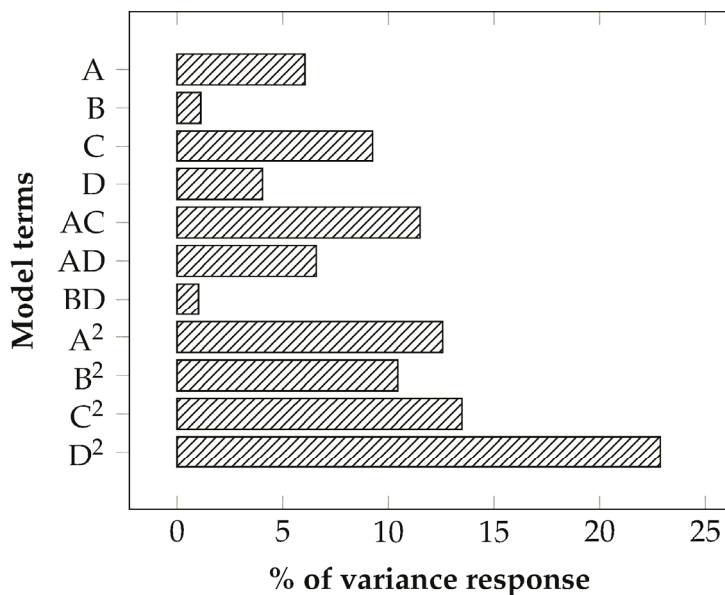
Figure 6. Proportionate contribution of each term of the quadratic model to the R^2 statistic.

3.6. Diagnostic

After the definition of the refined model, a diagnostic phase has been carried out in order to evaluate the assumptions at the basis of the procedure for the construction of the model by checking:

1. The normal distribution of the residuals
2. The absence of correlation of the residuals versus runs
3. The assumption of homoscedasticity (constant variance of the residuals)

The normal probability plot (Figure 7b) of the residuals seems to fit a straight line in quite a satisfactory manner. A more reliable way to have a statistical indication of this assumption has been found with the application of the Anderson-Darling test (ADT) [39].
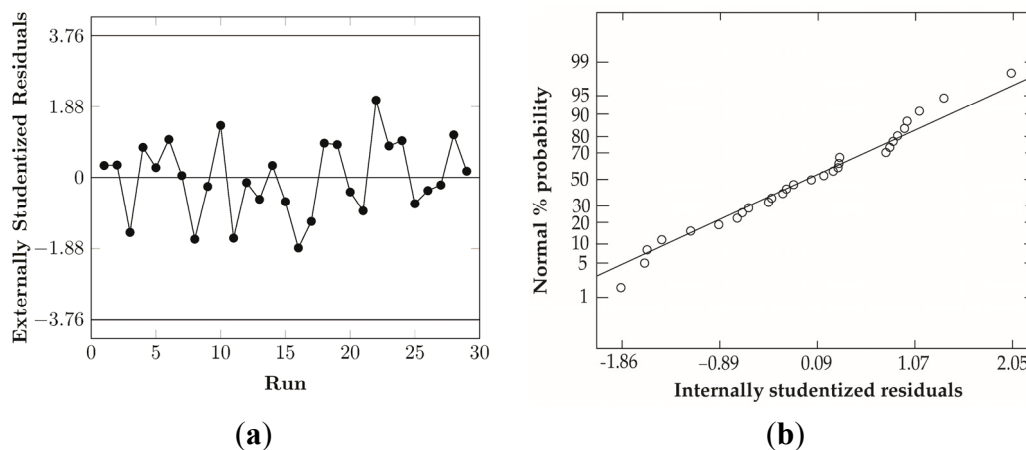
(a)
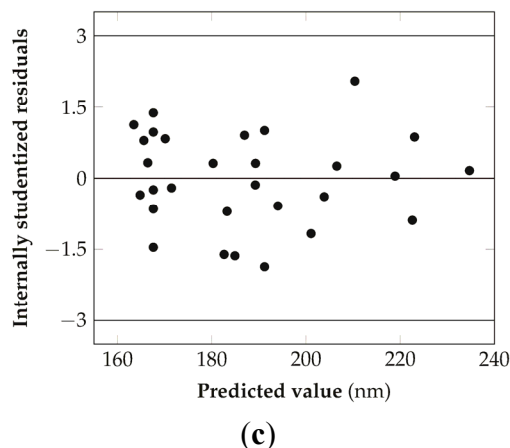
(b)

Figure 7. *Cont.*

(**c**)

Figure 7. Diagnostic plots for the check of the consistency of the model developed: (**a**) Residuals versus run for the check of the presence of time-related variable lurking in the background, (**b**) Normal probability plot for the check of the normal distribution of the residuals, (**c**) Residual versus predicted values plot for the check of the assumption of constant variance of the residuals.

This test can be used to quantify the deviation of a set of residuals from a given distribution. In this case it has been used to test the null hypothesis that the normal distribution adequately describes the residuals, using the comparison of the calculated statistics with a critical value at a 5% level of significance. For the present sample size of 29 residuals, the obtained p-value of 0.75 is higher than the cut-off value of 0.05, confirming the conclusion drawn from the visual inspection of the normal probability plot.

The assessment of the presence of autocorrelation in the residuals obtained from the linear regression was realized with the Durbin-Watson test [40,41]. In this case, the statistic is used to evaluate the null hypothesis that the residuals are not negatively nor positively correlated, at a 5% level of confidence. According to the formula, the value of the statistic always falls between 0 and 4, and a value of 2 indicates no presence of autocorrelation. In the present case the test gave a value of 1.99, which is very close to 2, and indicates no significant autocorrelation [42]. A second control can be done, visually, from the plot of the residuals versus the runs, which show no distinct increasing or decreasing pattern over time (Figure 7a). The plot of the residuals versus the predicted values (Figure 7c), for the assumption of the constant variance, doesn't seem to present a specific increasing or decreasing funnel pattern so the final model has been used without specific transformation of the data. In any case, a statistical evaluation of the homoscedasticity condition has been carried with the Levene's test [43] both for the residuals versus the predicted values and for the comparison of the residuals' variances at the different levels of each regressor. In the first case, the violation of this condition should provide a different spreading of the residuals along the predicted value axis and, to evaluate this, the interval has been divided into three parts of equal extension, the residuals of each interval have been grouped, and their variances tested against each other.

The resulting statistics give a value of 1.79 and a *p*-value of 0.4077 (higher than the threshold value of 0.05), according to which it is not possible to reject the null hypothesis of equal variances. In the second case, the test was applied by grouping the residuals according to the three different levels of the

regressors and the corresponding variances tested between each other. The results of the test (Table 7) reported a *p*-value higher than 0.05 for each of the regressors, excluding the possibility to reject the null hypothesis of equal variances.

Table 7. Summary of the Levene's test for the analysis of the homoscedasticity conditions of the residuals of the different levels of the model regressors.

Regressor	Levene's Statistic	*p*-Value
Sulfonation degree	4.907	0.086
Voltage	0.152	0.927
Distance	3.057	0.217
Flow-rate	0.603	0.740

3.7. Analysis of the Response Surface

From the polynomial model developed through the previous analysis it has been possible to construct the response surface to analyze the effect of the different variables on the final mean diameter of the nanofibers.

The relationship between the DS and the tip-to-collector distance in Figure 8 shows that a decrease of the mean diameter is accomplished by a combination of high sulfonation degrees and low distances, independently from the different levels of the voltage employed because of the statistical insignificance of the interaction terms AB and BC. For low sulfonation degrees, a possible improvement can be achieved at medium distances but the final dimension of the fibers are generally greater than those at high sulfonation degree for the same conditions of the other factors. However, this condition is verified for low-medium values of the flow-rate because, for the highest level, the minimum of the response surface shift towards the center of the design space, with a concurrent increment in the final mean fiber diameter.

A possible explanation can be related to the fact that an increase of the sulfonation degree of the material is capable to provide an increase in the conductivity of the solution in a similar way to the addition of a salt [20,44], leading to the formation of thinner fibers. Figure 9 presents the interaction between the sulfonation degree and the flow-rate. In this second case, better and more stable conditions are achieved by employing a low voltage coupled with low-medium distances, since the curvature of the response surface is less significant and it is possible to obtain lower mean fiber diameters for a wider range of flow rates and sulfonation degrees, with an higher flexibility of the process. This result can be ascribed to the fact that, in this condition, an optimal balance between electric field strength, solvent evaporation rate, and polymer jet stretching is achieved. For low flow rates the mean diameter increases probably due to a non-equilibrium condition between the flow rate and the jet removal from the tip which prevents the formation of a visible Taylor cone, with a more marked effect for low sulfonation degrees where the solution conductivity is lower. For higher distances the response surface is flatter and the mean diameter increases above the 200 nm. In the latter case, this effect is predominant on the different levels of the other variables involved, determining non optimal conditions for the production of thin fibers.
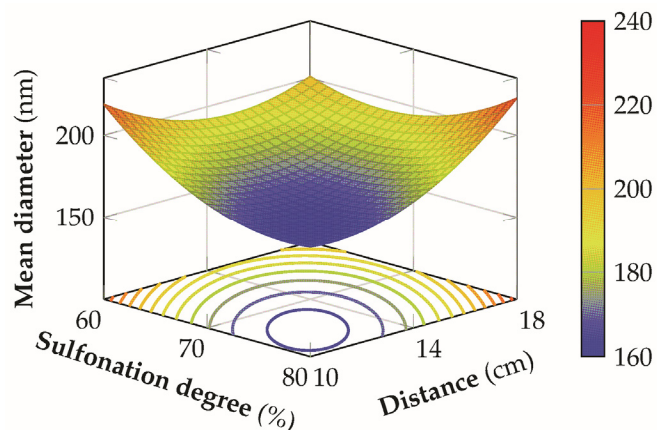
Figure 8. 3D response surface of the mean diameter for the sulfonation degree *versus* distance at an applied voltage of 25 kV and a flow-rate of 0.125 mL/h.
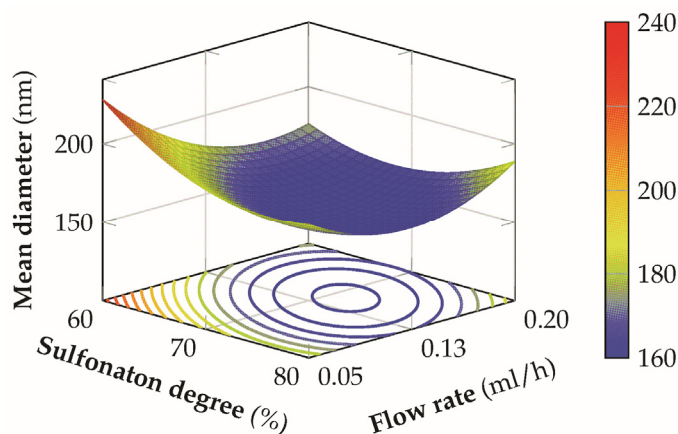

Figure 9. 3D response surface of the mean diameter for the sulfonation degree versus flow-rate at an applied voltage of 20 kV and at a distance of 14 cm.

The relationship between the voltage and the flow-rate, when the other variables at their medium values, is reported in Figure 10, from which it is possible to observe a saddle shape of the response surface. In this situation it is not possible to define unequivocally a specific optimal condition, but the contour plot of the response surface seems to suggest that, for a given flow rate, lower mean diameters could be obtained by operating with the lowest voltage value. The presence of a saddle shape of the response is not uncommon during the analysis of the relationship between these two factors [10] and several aspects need to be pointed out for the explanation of such behavior. An increment in the applied voltage, when all the other variables are held constant, is traduced in an increment in the mass flow rate ejected from the tip of the needle and a higher charge density. This induces an increment of the instability and stretching of the jet which could produce smaller fiber diameters. However discrepancies between the experimental results of several scientific works on the effect of the applied voltage for different polymer/solvent systems could suggest the necessity to include a concurrent effect of other variables, like feed rate and tip-to-collector distance, in the evaluation of such effect [45]. For the case in analysis the interaction shows more significant variation when the flow rate is changed for a fixed voltage, rather than the opposite case, stated the poor relevance of the voltage contribution term with respect to the flow rate, on the developed model.
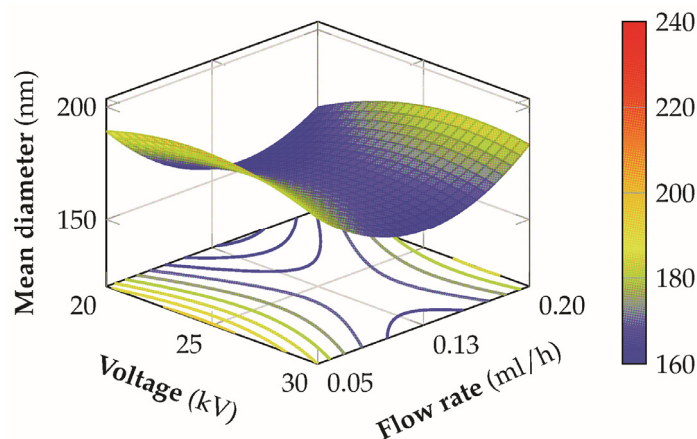
Figure 10. 3D response surface of the mean diameter for the voltage versus flow rate at a sulfonation degree of 70% and a distance of 14 cm from the tip to the needle.

3.8. Validation of the Model

Once analyzed, the behavior of the approximated response surface, in relation to the different levels of the variables involved in the design, the final step has been the validation of the obtained model. The objective of this validation has been to define constrained optimization conditions in order to obtain uniform and thin sPEEK nanofibers for samples at a given sulfonation degree and comparing the results from the values predicted by the software both in terms of mean diameter and standard deviation. In order to define optimal conditions for the standard deviation of the analyzed samples, a response surface was built based on a specific model developed for the data collected from the image analysis. In this second case a quadratic model was found to be adequate to describe the data with and R^2 value of 0.95.

The final equation excluded the presence of the voltage and showed the relevance of the interaction terms between the sulfonation degree with distance and flow rate, as in the case of the model for the mean diameter. The data have shown the presence of a positive correlation (correlation coefficient = 0.718) between the mean diameter and the standard deviation, showing a good chance to obtain similar conditions for the combined optimization. To this end, both the responses involved have been minimized using a desirability function, defined as:

$$D = \left[\prod_{i=1}^{N} d_i^{r_i} \right]^{1/\Sigma r_i} \tag{11}$$

where N is the number of responses, r_i is the value of the importance attributed to the selected response and d_i is the partial desirability function for specific responses. For the case in analysis, the relative importance selected was a value of 3 on a maximum value of 5, in order to set the optimization of the process by defining an equal importance for both the two responses. The numerical optimization has been carried via a penalty function approach using the downhill simplex method (Nelder-Mead method [46]) for multidimensional minimization. Three samples with different sulfonation degrees were selected and the relative optimized conditions were set for the electrospinning experiments (Table 8).

Table 8. Predicted optimized conditions and relative desirability function values for three samples at different sulfonation degrees.

Sample	Sulfonation Degree (%)	Voltage (kV)	Distance (cm)	Flow-Rate (mL/h)	Desirability
1	62	20	14.5	0.160	0.954
2	65	21	14.5	0.143	0.971
3	73	21	13.5	0.114	0.962

The results (Figure 11) have shown an acceptable accordance with the model prediction for the mean diameter and, to a less extent, for the standard deviation, probably due to the low value (0.88) of the predicted R^2 of the relative model.
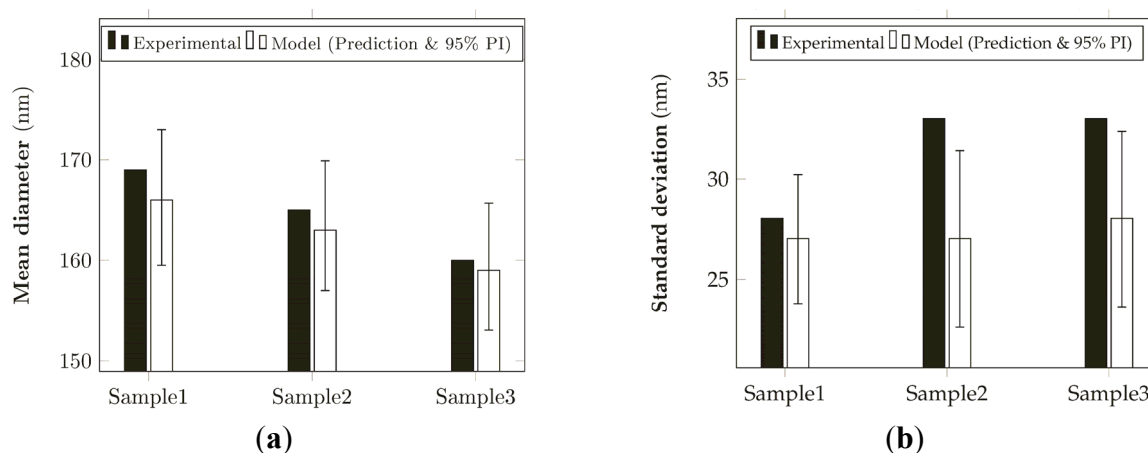
Figure 11. Comparison between the experimental results and the model prediction (prediction and 95% prediction interval) for: (**a**) the mean diameters and (**b**) the standard deviation of electrospun nanofibers.

4. Conclusions

Sulfonation of polyether ether ketone with concentrated sulfuric acid has been accomplished as a preliminary phase for the production of electrospun nanofibers for potential applications in the energy field. The reaction has been modeled with a suggested kinetic expression that takes into consideration a deflator effect of the sulfonated portion of the polymer, with a good fitting of the experimental data. The modified polymer can be completely solubilized in different organic aprotic solvents for medium degrees of sulfonation. The same solvents can be employed for the electrospinning of the material but with different ranges of concentration, according to their specific physical properties. A first screening activity has been carried out to select the proper set of variables for a subsequent, more careful, analysis using a DoE approach. The general conditions for the electrospinning of the material require high polymer concentrations, medium-high voltages, low flow-rates, and low relative humidity to allow a proper collection of the nanofibers. A more detailed analysis has been carried out to develop a model for the description of the response surface of the mean fiber diameter using a BBD in which both process (voltage, tip-to-collector distance, flow-rate) and material (sulfonation degree) factors have been taken into consideration. The developed model has shown a good descriptive capability of the observed data, the presence of interaction between sulfonation degree, and both the flow rate and the distance

parameters, while voltage has proven to have little or no effect on the final fibers dimensions. The model showed a good capability in the description of the selected response changes in the design space and it has been validated, in combination with a second model employed for the description of the standard deviation, using optimized conditions for samples at different sulfonation degrees. Good results have been obtained for the description of the first response while the standard deviation showed less accordance to the predicted values. In this manner, it has been possible to define optimized conditions in order to minimize the final mean diameter and standard deviation of the fibers according to the different values of the sulfonation degree in the range analyzed.

Author Contributions

Carlo Boaretti and Martina Roso conceived and designed the experiments. Carlo Boaretti performed the experiments. Carlo Boaretti, Martina Roso, Alessandra Lorenzetti and Michele Modesti analyzed and discussed the data. Carlo Boaretti wrote the manuscript with revisions by Michele Modesti, Martina Roso and Alessandra Lorenzetti.

Conflicts of Interest

The authors declare no conflict of interest.

References

1. Li, D.; Xia, Y. Electrospinning of nanofibers: reinventing the wheel? *Adv. Mater.* **2004**, *16*, 1151–1170.
2. Huang, Z.; Zhang, Y.; Kotaki, M.; Ramakrishna, S. A review on polymer nanofibers by electrospinning and their applications in nanocomposites. *Compos. Sci. Technol.* **2003**, *63*, 2223–2253.
3. Chronakis, I. Novel nanocomposites and nanoceramics based on polymer nanofibers using electrospinning process—A review. *J. Mater. Process. Tech.* **2005**, *167*, 283–293.
4. Dai, Y.; Liu, W.; Formo, E.; Sun, Y.; Xia, Y. Ceramic nanofibers fabricated by electrospinning and their applications in catalysis, environmental science, and energy technology. *Polym. Advan. Technol.* **2011**, *22*, 326–338.
5. Wu, H.; Zhang, R.; Liu, X.; Lin, D.; Pan, W. Electrospinning of Fe, Co, and Ni nanofibers: synthesis, assembly, and magnetic properties. *Chem. Mater.* **2007**, *19*, 3506–3511.
6. Sukigara, S.; Gandhi, M.; Ayutsede, J.; Micklus, M.; Ko, F. Regeneration of Bombyx mori silk by electrospinning. Part 2. Process optimization and empirical modeling using response surface methodology. *Polymer* **2004**, *45*, 3701–3708.
7. Gu, S.; Ren, J. Process Optimization and Empirical Modeling for Electrospun Poly(D,L-lactide) Fibers using Response Surface Methodology. *J. Macromol. Mater. Eng.* **2005**, *290*, 1097–1105.
8. Yördem, O.; Papila, M.; Menceloğlu, Y. Effects of electrospinning parameters on polyacrylonitrile nanofiber diameter: An investigation by response surface methodology. *Mater. Design* **2008**, *29*, 34–44.
9. Ray, S.; Lalman, J. Using the Box–Benkhen design (BBD) to minimize the diameter of electrospun titanium dioxide nanofibers. *Chem. Eng. J.* **2011**, *169*, 116–125.
10. Roso, M.; Lorenzetti, A.; Besco, S.; Monti, M.; Berti G.; Modesti, M. Application of empirical modelling in multi-layers membrane manufacturing. *Comput. Chem. Eng.* **2011**, *35*, 2248–2256.

11. Nasouri, K.; Bahrambeygi, H.; Rabbi, A.; Shoushtari, A.M.; Kaou, A. Modeling and optimization of electrospun PAN nanofiber diameter using response surface methodology and artificial neural networks. *J. Appl. Polym. Sci*. **2012**, *126*, 127–135.

12. Konwarh, R.; Misra, M.; Mohanty, A.K.; Karak, N. Diameter-tuning of electrospun cellulose acetate fibers: A Box–Behnken design (BBD) study. *Carbohyd. Polym*. **2013**, *92*, 1100–1106.

13. Kong, L.; Ziegler, G. Quantitative relationship between electrospinning parameters and starch fiber diameter. *Carbohyd. Polym*. **2013**, *92*, 1416–1422.

14. Wycisk, R.; Pintauro, P.N.; Park, J. New developments in proton conducting membranes for fuel cells. *Curr. Opin. Chem. Eng*. **2014**, *4*, 71–78.

15. Dong, B.; Gwee, L.; Salas-de la Cruz, D.; Winey, K.I.; Elabd, Y.A. Super proton conductive high-purity nafion nanofibers. *Nano Lett*. **2010**, *10*, 3785–3790.

16. Wang, W.; Li, Z.; Jiang, T.; Zhao, Z.; Li, Y.; Wang, Z.; Wang, C. sulfonated poly(ether ether ketone)/polypyrrole core-shell nanofibers: A novel polymeric adsorbent/conducting polymer nanostructures for ultra-sensitive gas sensors *ACS Appl. Mater. Inter*. **2012**, *4*, 6080–6084.

17. Lee, C.; Jo, S.; Choi, J.; Baek, K.; Truong, Y.; Kyratzis, I.; Shul, Y. SiO_2/sulfonated poly ether ether ketone (sPEEK) composite nanofiber mat supported proton exchange membranes for fuel cells. *J. Mater. Sci*. **2013**, *48*, 3665–3671.

18. Chakrabarty, T.; Kumar, M.; Rajesh, K.; Shahi, V.; Natarajan, T. Nano-fibrous sulfonated poly(ether ether ketone) membrane for selective electro transport of ions. *Sep. Purif. Technol*. **2010**, *75*, 174–182.

19. Choi, J.; Lee, C.; Hawkins, S.C.; Huynh, C.P.; Park, J.; Jeon, Y.; Truong, Y.B.; Kyratzis, I.L.; Shul, Y.G.; Caruso, R.A. Direct spun aligned carbon nanotube web-reinforced proton exchange membranes for fuel cells. *RSC Adv*. **2014**, *4*, 32787–32790.

20. Li, X.; Hao, X.; Na, H. Preparation of nanosilver particles into sulfonated poly(ether ether ketone) (S-PEEK) nanostructures by electrospinning. *Mater. Lett*. **2007**, *61*, 421–426.

21. Huang, R.Y.M.; Shao, P.; Burns, C.M.; Feng, X. Sulfonation of poly(ether ether ketone)(PEEK): kinetic study and characterization. *J. Appl. Polym. Sci*. **2001**, *82*, 2651–2660.

22. Jiang, R.; Kunz, H.; Fenton, J.M. Investigation of membrane property and fuel cell behavior with sulfonated poly(ether ether ketone) electrolyte: temperature and relative humidity effects. *J. Power Sources* **2005**, *150*, 120–128.

23. Gong, C.; Guan, R.; Shu, Y.; Chuang, F.; Tsen, W. Effect of sulfonic group on solubility parameters and solubility behavior of poly(2,6-dimethyl-1,4-phenylene oxide). *Polym. Adv. Technol*. **2007**, *18*, 44–49.

24. Box, G.; Behnken, D. Some new three level designs for the study of quantitative variables. *Technometrics* **1960**, *2*, 455–475.

25. Box, G.; Draper, N. Empirical Model-Building and Response Surfaces. In *Wiley Series in Probability and Statistics*; Wiley: New York, NY, USA, 1987.

26. Bishop, M.; Langley, K. Solubility and properties of a poly(aryl ether ketone) in strong acids. *Macromolecules* **1985**, *18*, 86–93.

27. Myers, R.; Montgomery, D.; Anderson-Cook, C. *Wiley Series in Probability and Statistics*; Wiley: Hoboken, NJ, USA, 2009.

28. Fong, H.; Chun, I.; Reneker, D. Beaded nanofibers formed during electrospinning. *Polymer* **1999**, *40*, 4585–4592.

29. Deitzel, J.; Kleinmeyer, J.; Harris, D.; Beck Tan, N.C. The effect of processing variables on the morphology of electrospun nanofibers and textiles. *Polymer* **2001**, *42*, 261–272.

30. Lee, K.; Kim, H.; Bang, H.; Jung, Y.; Lee, S. The change of bead morphology formed on electrospun polystyrene fibers. *Polymer* **2003**, *44*, 4029–4034.

31. Cerfontain, H. Mechanistic aspects in aromatic sulfonation and desulfonation. In *Interscience Monographs on Organic Chemistry Series*; Interscience Publishers: New York, NY, USA, 1968.

32. Compton, R.; Bamford, C.; Tipper, C. Reaction of aromatic compounds. In *Comprehensive Chemical Kinetics: Volume 13*; Elsevier: Amsterdam, The Netherland, 1972.

33. Kučera, F.; Jančar, J. Homogeneous and heterogeneous sulfonation of polymers: A review. *Polym. Eng. Sci.* **1998**, *38*, 783–792.

34. Shibuya, N.; Porter, R. Kinetics of PEEK sulfonation in concentrated sulfuric acid. *Macromolecules* **1992**, *25*, 6495–6499.

35. Shibuya, N.; Porter, R. A reconsideration of the kinetics of aromatic sulfonation by sulfuric acid. *Macromolecules* **1994**, *27*, 6267–6271.

36. Subramanian, C.; Weiss, R.; Shaw, M.T. Electrospinning and characterization of highly sulfonated polystyrene fibers. *Polymer* **2010**, *51*, 1983–1989.

37. Okuzaki, H.; Takahashi, T.; Miyajima, N.; Suzuki, Y.; Kuwabara, T. Spontaneous formation of Poly(p-phenylenevinylene) nanofiber yarns through electrospinning of a precursor. *Macromolecules* **2006**, *39*, 4276–4278.

38. Laforgue, A.; Robitaille, L.; Mokrini, A.; Ajji, A. Fabrication and characterization of ionic conducting nanofibers. *Mater. Eng.* **2006**, *292*, 1229–1236.

39. Anderson, T.; Darling, D. Asymptotic theory of certain goodness-of-fit criteria based on stochastic processes. *Ann. Math. Statistics* **1952**, *23*, 193–212.

40. Durbin, J.; Watson, G. Testing for serial correlation in least squares regression, I. *Biometrika* **1950**, *37*, 409–428.

41. Durbin, J.; Watson, G. Testing for serial correlation in least squares regression, II. *Biometrika* **1951**, *38*, 159–179.

42. Yetilmezsoy, K.; Demirel, S.; Vanderbei, R. Response surface modeling of Pb(II) removal from aqueous solution by Pistacia vera L.: Box-Behnken experimental design. *J. Hazard. Mater.* **2009**, *171*, 551–562.

43. Levene, H. Robust tests for equality of variances. In *Contributions to Probability and Statistics*; Stanford University Press: Stanford, CA, USA, 1960.

44. Li, X.; Hao, X.; Xu, D.; Zhang, G.; Zhong, S.; Na, H.; Wang, D. Fabrication of sulfonated poly(ether ether ketone ketone) membranes with high proton conductivity. *J. Membrane Sci.* **2006**, *281*, 1–6.

45. Andrady, A. *Science and Technology of Polymer Nanofibers*; Wiley: Hoboken, NJ, USA, 2008.

46. Press, W.H.; Flannery, B.P.; Teukolsky, S.A.; Vetterling, W.T. *Numerical Recipes in Pascal: The Art of Scientific Computing*; Cambridge University Press: New York, NY, USA, 1989.